Mössbauer spectral evidence for rhombohedral symmetry in $R_3Fe_5O_{12}$ garnets with R = Y, Eu and Dy

2001 J. Phys.: Condens. Matter 13 1759

(http://iopscience.iop.org/0953-8984/13/8/312)

INSTITUTE OF PHYSICS PUBLISHING JOURNAL OF PHYSICS: CONDENSED MATTER

J. Phys.: Condens. Matter **13** (2001) 1759–1772 www.iop.org/Journals/cm PII: S0953-8984(01)18267-6

Mössbauer spectral evidence for rhombohedral symmetry in $R_3Fe_5O_{12}$ garnets with R = Y, Eu and Dy

D Vandormael[1], F Grandjean[1], Dimitri Hautot[2] and Gary J Long[2]

[1] Insitut de Physique B5, Université de Liège, B-4000 Sart-Tilman, Belgium
[2] Department of Chemistry, University of Missouri–Rolla, Rolla, MO 65409-0010, USA

Received 18 October 2000

Abstract

The iron-57 Mössbauer spectra of $R_3Fe_5O_{12}$, where R is Y, Eu and Dy, have been measured between 4.2 and 550 K. The substantial quadrupole splittings observed in the paramagnetic spectra confirm that the local symmetry at both the tetrahedral and octahedral iron(III) sites is not cubic. The low temperature Mössbauer spectra of $Dy_3Fe_5O_{12}$ clearly confirm the spin reorientation between 10 and 15 K and the 4.2 and 10 K spectra are consistent with the known orientation of the magnetization at 14 K in the cubic $Ia\bar{3}d$ unit cell. The Mössbauer spectra of $R_3Fe_5O_{12}$, where R is Y, Eu and Dy, obtained between 45 and 295 K, reveal four different tetrahedral iron(III) Mössbauer spectral components, four components which are inconsistent with a magnetization oriented along the [111] axis of a cubic $Ia\bar{3}d$ unit cell. In contrast, these four components are consistent with a crystal symmetry which is reduced from cubic to rhombohedral $R\bar{3}$. The temperature dependence of the hyperfine fields in $Dy_3Fe_5O_{12}$ indicates a small biquadratic exchange contribution to the magnetic exchange. The temperature dependence of the isomer shifts in $Dy_3Fe_5O_{12}$ gives Mössbauer lattice temperatures of 405 and 505 K for the 16a and 24d sites, respectively, values which are in excellent agreement with the Debye temperature measured for $Y_3Fe_5O_{12}$.

1. Introduction

The recent multimedia revolution has increased the need for new higher density recording media. The new blue laser diodes permits us to increase the density of recording media by a factor of four as compared with media which use the conventional red laser. However, the implementation of these improvements requires magneto-optical materials with a high efficiency in the blue region of the visible spectrum. Thin films of rare-earth iron garnets with the general formula $R_3Fe_5O_{12}$ and, more specifically, their partially substituted $(Bi, Dy)_3(Fe, Ga)_5O_{12}$ solid solutions, are the most viable candidates for the next generation of efficient magneto-optical media [1, 2].

Recent studies [3, 4] by x-ray and neutron diffraction of the dysprosium, holmium and terbium iron garnets indicate that, both in their paramagnetic and ferrimagnetic states, they

crystallize in the cubic $Ia\bar{3}d$ structure. However, in the past several authors have proposed [5–8] that rare-earth iron garnets undergo a rhombohedral distortion below their Curie temperatures.

In the cubic $Ia\bar{3}d$ space group the trivalent rare-earth ions occupy the 24c dodecahedral site and the trivalent iron ions occupy the 16a octahedral and 24d tetrahedral sites. In these two sites the iron(III) ions are surrounded by oxygen dianions, which form [9] distorted octahedra and tetrahedra, respectively, and, as a consequence, the local symmetry at the iron(III) sites is not cubic. Indeed, if the oxygen tetrahedra are inscribed within a cube whose axes are parallel to the unit cell axes, the tetrahedra are elongated along one of their three S_4 axes, an axis which coincides with the [001] edge of the unit cell; the tetrahedra are thus rotated alternately through an angle of $+16^\circ$ or -16° about the [100] direction. In contrast, the oxygen octahedra are elongated along one of their four S_6 axes, an axis which coincides with the [111] direction of the cubic unit cell and is rotated alternately through an angle of $+28^\circ$ or -28° about the [111] direction. Two tetrahedron edge lengths of 3.16 and 2.87 Å and two octahedron edge lengths of 2.68 and 2.99 Å have been observed [10] in $Y_3Fe_5O_{12}$. These different lengths clearly reflect substantial local deviation from a cubic environment at the iron sites.

The rare-earth iron garnets are ferrimagnetic compounds [10, 11], in which the two inequivalent 16a and 24d iron(III) sites are antiferromagnetically coupled and, for the heavier rare-earth ions, the resultant net iron moment is antiferromagnetically coupled with the 24c rare-earth magnetic moment. The magnetization is usually oriented [12] along the [111] direction of the cubic unit cell, but spin reorientations occur [13, 14] at low temperature, as will be discussed below for $Dy_3Fe_5O_{12}$. The opposed net iron and rare-earth magnetic moments compensate each other at the compensation temperature, a temperature which can be varied through an appropriate substitution of the trivalent rare-earth ion, in order to satisfy specific technological requirements. In contrast, Curie temperatures of the various rare-earth iron garnets, which are typically 550 K, are determined, to a first approximation, by the iron sublattice coupling and, hence, they are essentially independent of the nature of the rare-earth ion present.

In spite of the incompatibility between the perfect cubic $Ia\bar{3}d$ structure and the alignment of the magnetization along the [111] axis of this structure, x-ray and neutron diffraction studies have failed [3, 13] to reveal any substantial departure from a cubic structure, i.e., any rhombohedral distortion.

There have been a number of earlier Mössbauer spectral studies [15–19] of the $R_3Fe_5O_{12}$ garnets but, in general, these spectra are of surprisingly poor quality. Hence, high quality data are required to investigate both the local structural and magnetic properties of the garnets. In this paper high resolution Mössbauer spectra of $R_3Fe_5O_{12}$, where R is Y, Eu and Dy, obtained at various temperatures between 4.2 and 550 K, are analysed in terms of a model which clearly indicates a rhombohedral distortion of these compounds below their Curie temperatures. Further, the analysis of these spectra will help in understanding the conversion electron Mössbauer spectra [20] of sputtered garnet films, the films which are potentially important as new recording media.

2. Experiment

Stoichiometric mixtures of 1.5 moles of R_2O_3, where R is Y, Eu and Dy, and 5 moles of $FeC_2O_4 \cdot 2H_2O$ are ground in an agate mortar. This mixture is dissolved in an excess of 65% HNO_3 at 473 K. The dry residue is heated from room temperature to 1473 K in six ten hour steps of 200 K and then maintained at 1473 K for 48 hours. The samples were ground between each ten hour step to eliminate any carbonate and nitrate salts and to ensure sample homogeneity.

X-ray diffraction patterns indicate that the samples have the cubic $Ia\bar{3}d$ structure, and the lattice parameters obtained from these patterns agree with the literature [21] values. No

$RFeO_3$ orthoferrite phase is detected by x-ray diffraction in any of the samples. However, the sample of $Y_3Fe_5O_{12}$ contains ∼5% of Fe_2O_3, an impurity which is easily detected and fitted in the Mössbauer spectra.

Mössbauer spectral absorbers of 6 to 10 mg cm^{-2} were prepared from powdered samples which had been sieved to a 0.045 mm or smaller diameter particle size. For measurements below room temperature the powdered sample was mixed with Vaseline, whereas for measurements above room temperature the powdered sample was mixed with boron nitride. The Mössbauer spectra were obtained between 4.2 and 550 K on a constant-acceleration spectrometer, which utilized a rhodium matrix cobalt-57 source and was calibrated at room temperature with α-iron foil. The studies between 4.2 and 295 K were carried out in a Janis Supervaritemp cryostat. The accuracy of the temperature is ±0.25 K. The studies between 295 and 550 K were carried out in an Austin Science Associates vacuum oven and the temperature was measured with an accuracy of ±3 K. The spectra have been fitted as discussed below and the estimated errors are at most ±0.1 kOe for the hyperfine fields, ±0.002 mm s^{-1} for the isomer shifts and ±0.01 mm s^{-1} for the quadrupole shifts.

3. Mössbauer spectral results

3.1. Paramagnetic Mössbauer spectra

The Mössbauer spectrum of $Dy_3Fe_5O_{12}$ obtained at 550 K, i.e., in the paramagnetic phase, is shown in figure 1. The substantial quadrupole splittings indicate that both the tetrahedral and octahedral iron site symmetries are not cubic as discussed in the introduction. This spectrum has been fitted with two symmetric Lorentzian doublets assigned to the 16a and 24d sites with relative areas constrained to 16:24 and with a single common width of 0.26 mm s^{-1}. Although two models [22], which differ in the relative positions of the two lines at ∼0.4 mm s^{-1}, successfully fit the 550 K spectrum, the model shown in figure 1 was chosen because the isomer shifts and quadrupole splittings, which are given in table 1, agree best with their temperature dependence as observed, see below, between 4.2 and 550 K.

Similar results were obtained on $Y_3Fe_5O_{12}$ above its Curie temperature and the hyperfine parameters resulting from a fit identical to that described for $Dy_3Fe_5O_{12}$ are also given in table 1. The isomer shifts and quadrupole splittings are in reasonable agreement with those obtained [15, 23] for substituted yttrium iron garnets.

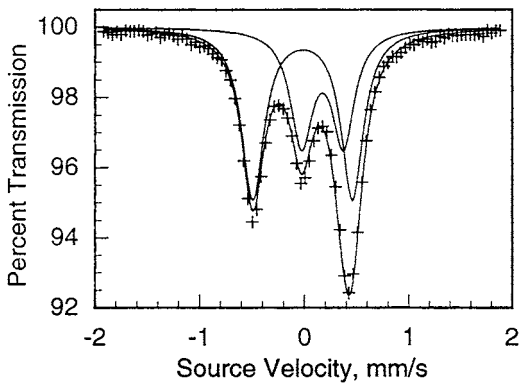

Figure 1. Mössbauer spectrum of $Dy_3Fe_5O_{12}$ obtained at 550 K.

Table 1. Mössbauer spectral parameters for $R_3Fe_5O_{12}$ obtained between 15 and 550 K.

R	Site	Parameter	15 K	45 K	85 K	150 K	200 K	250 K	295 K	550 K
Dy	16a	δ[a] (mm s^{-1})	0.495	0.493	0.490	0.465	0.435	0.413	0.382	0.173
		ΔE_Q (mm s^{-1})	−0.34	−0.34	−0.34	−0.34	−0.34	−0.34	−0.34	0.40
	$16a_{12}$	H (kOe)	548.4	548.0	545.3	535.4	525.0	508.2	492.1	—
	$16a_{12}$	θ[b](°)	70.5	70.5	70.5	70.5	70.5	70.5	70.5	—
	$16a_4$	H (kOe)	537.3	536.5	536.2	527.5	516.6	500.4	485.5	—
	$16a_4$	θ[b](°)	0	0	0	0	0	0	0	—
	24d	δ[a] (mm s^{-1})	0.265	0.270	0.254	0.232	0.213	0.188	0.155	−0.015
		ΔE_Q (mm s^{-1})	−0.99	−0.99	−0.99	−0.99	−0.99	−0.99	−0.99	0.95
	$24d_{6,1}$	H (kOe)	478.8	475.3	472.8	458.0	439.3	418.0	401.2	—
	$24d_{6,1}$	θ(°)	61	62	67	70	68	68	69	—
	$24d_{6,2}$	H (kOe)	481.5	475.7	473.9	462.2	442.1	420.6	403.2	—
	$24d_{6,2}$	θ(°)	47	47	45	46	50	50	50	—
	$24d_{6,3}$	H (kOe)	470.5	469.9	463.9	445.6	434.0	414.3	393.2	—
	$24d_{6,3}$	θ(°)	47	47	45	44	46	46	46	—
	$24d_{6,4}$	H (kOe)	469.7	466.2	462.0	445.5	433.8	413.5	391.4	—
	$24d_{6,4}$	θ(°)	61	62	66	68	60	60	60	—
Y	16a	δ[a] (mm s^{-1})	—	—	0.486	0.466	0.445	0.416	0.383	0.096
		ΔE_Q (mm s^{-1})	—	—	−0.37	−0.37	−0.37	−0.37	−0.37	0.37
	$16a_{12}$	H (kOe)	—	—	545.2	538.0	527.0	512.0	491.0	—
	$16a_{12}$	θ[b](°)	—	—	70.5	70.5	70.5	70.5	70.5	—
	$16a_4$	H (kOe)	—	—	540.3	532.5	521.0	506.5	486.0	—
	$16a_4$	θ[b](°)	—	—	0	0	0	0	0	—
	24d	δ[a] (mm s^{-1})	—	—	0.252	0.236	0.214	0.188	0.153	−0.077
		ΔE_Q (mm s^{-1})	—	—	−1.00	−1.00	−1.00	−1.00	−1.00	1.00
	$24d_{6,1}$	H (kOe)	—	—	467.4	458.4	441.2	422.0	398.7	—
	$24d_{6,1}$	θ(°)	—	—	56	56	56	56	56	—
	$24d_{6,2}$	H (kOe)	—	—	462.6	448.4	435.8	415.5	385.7	—
	$24d_{6,2}$	θ(°)	—	—	54	54	54	54	54	—
	$24d_{6,3}$	H (kOe)	—	—	465.4	455.4	439.0	419.6	400.7	—
	$24d_{6,3}$	θ(°)	—	—	44	44	40	40	45	—
	$24d_{6,4}$	H (kOe)	—	—	464.8	453.5	437.9	418.4	395.8	—
	$24d_{6,4}$	θ(°)	—	—	72	70	72	75	75	—
Eu	16a	δ[a] (mm s^{-1})	—	—	0.505	0.480	0.460	0.423	0.400	
		ΔE_Q (mm s^{-1})	—	—	−0.26	−0.26	−0.26	−0.26	−0.26	
	$16a_{12}$	H (kOe)	—	—	547.2	536.9	526.9	515.0	495.5	—
	$16a_{12}$	θ[b](°)	—	—	70.5	70.5	70.5	70.5	70.5	—
	$16a_4$	H (kOe)	—	—	541.2	530.7	521.0	507.0	492.0	—
	$16a_4$	θ[b](°)	—	—	0	0	0	0	0	—
	24d	δ[a] (mm s^{-1})	—	—	0.278	0.255	0.232	0.200	0.177	—
		ΔE_Q (mm s^{-1})	—	—	−0.97	−0.97	−0.97	−0.97	−0.97	—
	$24d_{6,1}$	H (kOe)	—	—	470.6	457.0	443.7	426.5	401.9	—
	$24d_{6,1}$	θ(°)	—	—	66	72	64	64	64	—
	$24d_{6,2}$	H (kOe)	—	—	466.3	457.8	441.0	424.0	401.0	—
	$24d_{6,2}$	θ(°)	—	—	44	44	48	48	46	—
	$24d_{6,3}$	H (kOe)	—	—	472.3	453.3	439.6	422.7	399.2	—
	$24d_{6,3}$	θ(°)	—	—	50	50	54	54	54	—
	$24d_{6,4}$	H (kOe)	—	—	463.1	453.3	437.8	416.8	404.5	—
	$24d_{6,4}$	θ(°)	—	—	60	60	56	56	56	—

[a] Relative to room temperature α-iron foil.
[b] These θ values have been held constant, see text.

3.2. Magnetic Mössbauer spectra obtained below 15 K

The Mössbauer spectra of $Dy_3Fe_5O_{12}$, obtained at 4.2, 10 and 15 K, are shown in figure 2. From magnetic torque measurements, Aubert and Michelutti [14] concluded that, below 14 K, the magnetization makes an angle of 17° with the [111] axis of each (110) plane of the cubic unit cell, whereas above 14 K, it is parallel to the [111] axis. This spin reorientation is evidenced by differences between the spectra at 10 and 15 K, mainly in the shape of the absorption lines at ~ -7.5, -4.4 and 8 mm s^{-1}.

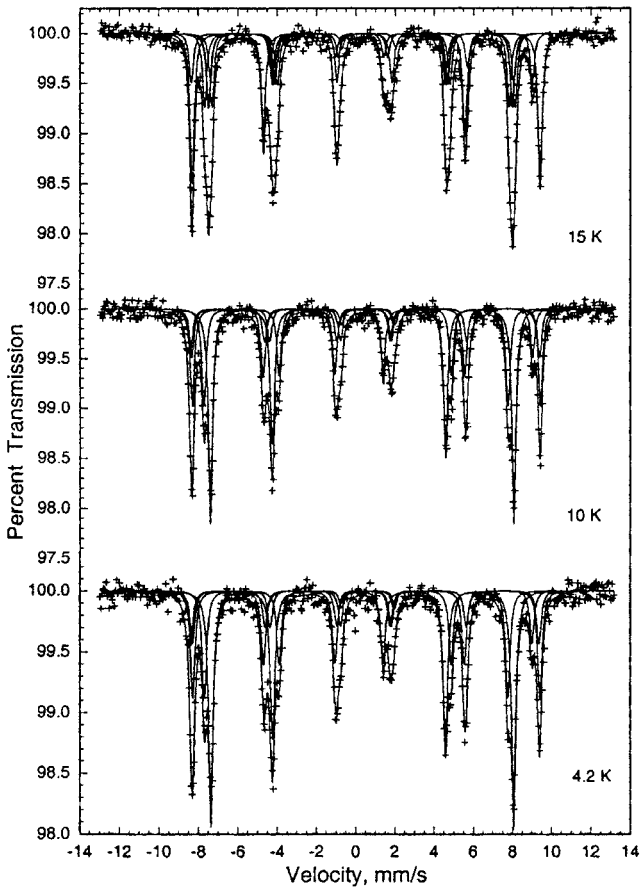

Figure 2. Mössbauer spectra of $Dy_3Fe_5O_{12}$ obtained at 4.2, 10 and 15 K.

Below 14 K the orientation of the magnetization and, hence, of the iron magnetic moments relative to the principal axis of the electric field gradient tensor of the 16a and 24d sites, gives rise in the Mössbauer spectra to three magnetically inequivalent 16a sites, labelled herein $16a_8$, $16a_{4,1}$, and $16a_{4,2}$, and two magnetically inequivalent 24d sites, labelled herein $24d_{16}$ and $24d_8$. As a consequence, the Mössbauer spectra at 4.2 and 10 K, see figure 2, have been fitted with three sextets, with an area ratio of 8:4:4, assigned to the $16a_8$, $16a_{4,1}$ and $16a_{4,2}$ sites, and two sextets, with an area ratio of 16:8, assigned to the $24d_{16}$ and $24d_8$ sites. The isomer shifts and the quadrupole interactions, $e^2Qq/2$, of the crystallographically equivalent but magnetically inequivalent sites were constrained to be equal and to be consistent with their values observed above 10 K, see below. The values of the θ angles between the magnetization, and hence the

Table 2. Mössbauer spectral parameters for $Dy_3Fe_5O_{12}$ obtained at low temperatures.

Site	Parameter	4.2 K	10 K
16a	δ^2 (mm s^{-1})	0.495	0.495
	ΔE_Q (mm s^{-1})	−0.32	−0.32
$16a_8$	H (kOe)	548.0	549.0
$16a_8$	θ^b(°)	79.71	79.71
$16a_{4,1}$	H (kOe)	535.3	537.2
$16a_{4,1}$	θ^b(°)	17.25	17.25
$16a_{4,2}$	H (kOe)	549.3	551.0
$16a_{4,2}$	θ^b(°)	53.28	53.28
24d	δ^a (mm s^{-1})	0.260	0.255
	ΔE_Q (mm s^{-1})	−0.99	−0.99
$24d_{16}$	H (kOe)	474.4	475.2
$24d_{16}$	θ(°)	62.70	62.70
$24d_8$	H (kOe)	475.3	476.1
$24d_8$	θ(°)	36.70	36.70

[a] Relative to room temperature α-iron foil.
[b] These θ values have been held constant.

hyperfine field, and the principal axis of the electric field gradient tensor were adjusted. The values found for the $16a_8$, $16a_{4,1}$, $16a_{4,2}$, $24d_{16}$ and $24d_8$ sites, are given in table 2 and are in agreement with the orientation of the magnetization proposed by Aubert and Michelutti [14]. A total of nine hyperfine parameters, a single common width of 0.26 mm s^{-1}, and the total absorption area were fit. The best fit values of the hyperfine parameters are given in table 2.

3.3. Magnetic Mössbauer spectra obtained between 15 and 285 K

The Mössbauer spectra of $R_3Fe_5O_{12}$, where R is Y, Eu and Dy, obtained at 85 and 295 K are shown in figures 3 and 4, respectively. It is obvious that the overall shapes of all the spectra are essentially independent of the nature of the rare-earth ion and that the average hyperfine field decreases slightly with increasing temperature.

If the magnetization and, hence, the hyperfine fields are orientated along the [111] direction of the $Ia\bar{3}d$ cubic unit cell, two magnetically inequivalent octahedral sites, herein labelled $16a_{12}$ and $16a_4$, and one tetrahedral site, 24d, are expected. As a consequence, at least three sextets would be required to fit the spectra between 15 and 295 K. Two sextets with the same isomer shift and the same quadrupole interaction, but different hyperfine fields and different θ angles of 70.5 and 0°, in the area ratio 12:4, are assigned to the $16a_{12}$ and $16a_4$ sites and one sextet with a θ angle of 54.7° and a relative area of 24 is assigned to the 24d site. Indeed, the contributions of the octahedral, $16a_{12}$ and $16a_4$, sites to the spectra are well modelled by two sextets with the above characteristics, as is shown in figures 3 and 4. This is easily observed for the lowest and highest velocity spectral lines at ~ -8.2 and 9.2 mm s^{-1}, respectively. However, it is *not* possible to fit the spectral contribution of the tetrahedral 24d site with only one sextet, even if a line width of 0.54 mm s^{-1} is used. Indeed, the absorption lines at ~ -7.2 and -4 mm s^{-1} are clearly broader than the octahedral absorption lines and reveal significant structure. Hence, their fit requires the use of several sextets. In cubic $Ia\bar{3}d$ symmetry, the broadening of the tetrahedral absorption lines could result [16] from a random distribution of the magnetization direction around the [111] direction, but such a distribution would also result in a broadening of the octahedral absorption lines, a broadening which is not observed. As we will show below, if there is no rhombohedral distortion of the unit cell below the Curie temperature, the

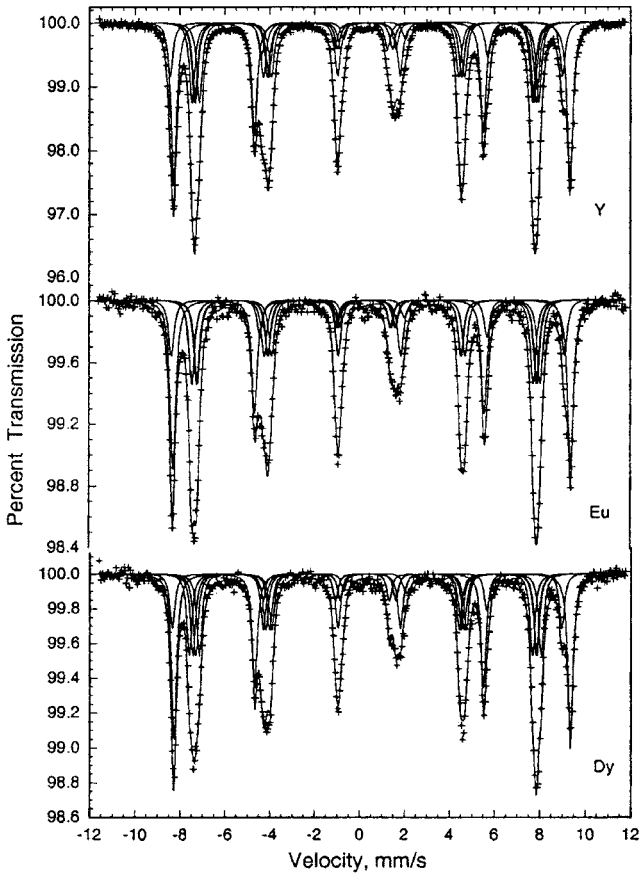

Figure 3. Mössbauer spectra of $R_3Fe_5O_{12}$, where R is Y, Eu and Dy, obtained at 85 K.

broadening and the shape of the tetrahedral absorption lines cannot be understood.

Because of the obvious broadening of the tetrahedral spectral absorption lines, we have attempted to model the tetrahedral absorption with two, three and four sextets [20]. Further, because the broadening of the low and high velocity lines of this component are different, it is not possible to fit the spectra with a distribution of only one hyperfine parameter, i.e., the hyperfine field or the θ angle. The physically reasonable four sextet model, shown in figures 3 and 4, successfully fits the Mössbauer spectra of $R_3Fe_5O_{12}$, where R is Y, Eu and Dy, obtained between 15 and 295 K and the resulting hyperfine parameters are given in table 1. In this model the four sextets assigned to the $24d_{6,1}$, $24d_{6,2}$, $24d_{6,3}$ and $24d_{6,4}$ sites have the same isomer shift and the same quadrupole interaction, different hyperfine fields and different θ angles and are in the fixed area ratio of 6:6:6:6. A total of 16 parameters, two isomer shifts, two quadrupole interactions, six hyperfine fields, four θ angles, a single common width and one total absorption area, were adjusted to obtain the fits shown in figures 3 and 4. The single common line widths are 0.29, 0.29 and 0.27 mm s^{-1} for the Y, Eu and Dy garnets, respectively, at all temperatures. Further, it should be noted that the line widths in the magnetic and paramagnetic spectra of $Dy_3Fe_5O_{12}$ are not significantly different.

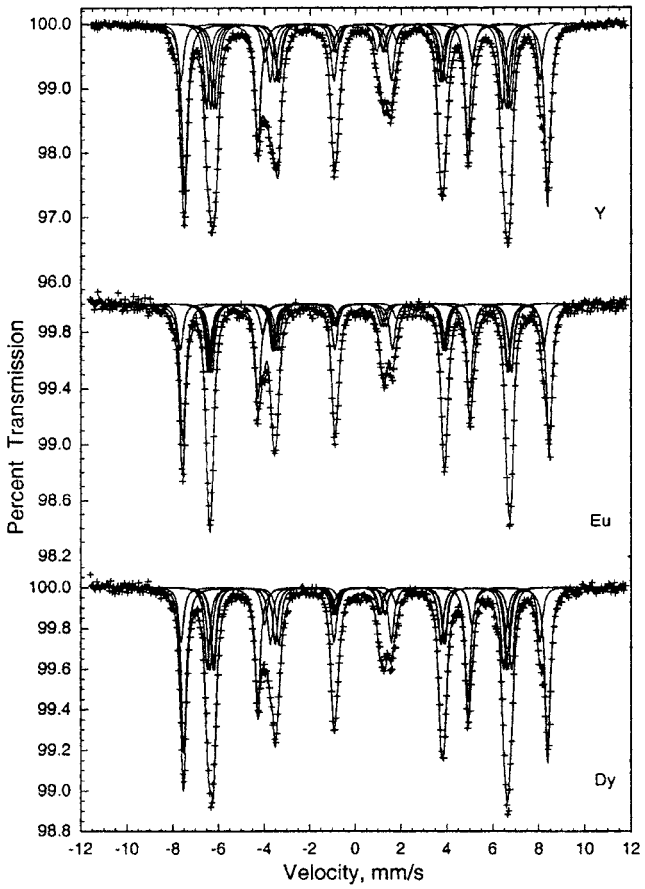

Figure 4. Mössbauer spectra of $R_3Fe_5O_{12}$, where R is Y. Eu and Dy, obtained at 295 K.

4. Discussion

4.1. Assignment of the sextets

Very early and/or poorly resolved Mössbauer spectra [16–18] of $Y_3Fe_5O_{12}$ were analysed in terms of two broad sextets assigned to the 16a and 24d sites, a model which has no physical justification. Other early Mössbauer spectra [15, 19] of $Y_3Fe_5O_{12}$ were analysed with three sextets, two assigned to the $16a_{12}$ and $16a_4$ sites and one assigned to the 24d site, an assignment which is in agreement with the cubic $Ia\bar{3}d$ structure. However, the limited resolution of these earlier spectra, i.e., approximately eight to ten data points per absorption line, does not permit the observation of any detailed fine structure in the 24d absorption lines. Later work [24] indicated that the 24d contribution to the spectra was not a simple sextet and it was fitted with two broad sextets, in a rather arbitrary fashion which again had no physical meaning.

Our high resolution spectra, with at least 16 data points per absorption line, see figures 3 and 4, clearly indicate that the 24d contribution to the spectra cannot be fit with one sextet. However the spectra are well fitted with four sextets with equal relative areas assigned to the four components resulting from the distortion of the tetrahedral 24d site. This model uses a large number of constraints, such as the same isomer shift and quadrupole interaction for the four components of the tetrahedral site, hyperfine fields differing by a small amount, and

different θ angles distributed around the expected magic angle of 54.7° for the cubic $Ia\bar{3}d$ structure. Further, the values of the isomer shift and quadrupole interaction are compatible with their paramagnetic values. Hence, the analysis presented herein in terms of two 16a and four 24d sextets may be understood if, within the cubic $Ia\bar{3}d$ structure, there are random local distortions, particularly around the 24d sites, distortions which would rotate the principal axis of the electric field gradient tensor relative to the [111] direction and, hence, give rise to the four different θ angles.

However, a more attractive explanation resides in the reduction of the unit-cell symmetry from cubic to rhombohedral. Single crystal x-ray structural data [8] and x-ray absorption fine structure spectra [25] of $Y_3Fe_5O_{12}$ were analysed in terms of a rhombohedral $R\bar{3}$ structure. In reducing the space group symmetry [8] from $Ia\bar{3}d$ to $R\bar{3}$, the 16a sites become the 1a, 1b, 2c, 3d, 3e and 6f sites and the 24d sites become four different 6f sites. This lowering of symmetry has been attributed [25] to an interchange of approximately two rare-earth 24c ions and two iron 16a ions per cubic unit cell. However, our Mössbauer spectra do not reveal the presence of any iron(III) ions on the dodecahedral 24c site, a presence which would appear as an additional sextet in the spectra with a relative area of 5%. In addition, the relative absorption area assigned to the 16a sites agrees exactly with the crystallographic degeneracy of the sites. Nevertheless, our analysis of the Mössbauer spectra of the $R_3Fe_5O_{12}$ compounds below their Curie temperatures can be understood in terms of the $R\bar{3}$ symmetry. The four sextets assigned to the tetrahedral 24d sites are easily assigned to the four different 6f sites. The six 1a, 1b, 2c, 3d, 3d and 6f sites can be grouped into two groups, first the 1a, 1b and 2c sites with the $\bar{3}$, $\bar{3}$ and 3 point symmetries, respectively, and second the 3d, 3e and 6f sites with the $\bar{1}$, $\bar{1}$ and 1 point symmetries, respectively. The first group would give rise to the $16a_4$ sextet and the second group to the $16a_{12}$ sextet. The displacements [8, 24] of the ions in going from the $Ia\bar{3}d$ to the $R\bar{3}$ space group are very small and, hence, the differences between the four sextets assigned to the four different 6f sites and the differences between the two $16a_4$ and $16a_{12}$ sextets are expected to be small, as in indicated by the values given in table 1. In the following discussion, we will however continue referring to the 16a and 24d sites, for the sake of notational simplicity.

4.2. Hyperfine fields

The temperature dependence of the site weighted average 16a and 24d hyperfine fields in $R_3Fe_5O_{12}$, where R is Y, Eu and Dy, is shown in figure 5. In general, the hyperfine fields are slightly larger in $Eu_3Fe_5O_{12}$, in agreement with its slightly larger unit-cell volume and are slightly smaller in $Y_3Fe_5O_{12}$, where Y is non-magnetic. In the three garnets, the octahedral 16a hyperfine field is larger than the tetrahedral 24d hyperfine field, in agreement with the higher covalency [26] of the iron(III) at the tetrahedral 24d site. More specifically, the increased covalency increases the 4s electron density at the iron nucleus and, consequently, decreases both the hyperfine field and the isomer shift, see below, at the tetrahedral site as compared to the octahedral site. This general trend is observed [26] in both spinels and garnets.

The temperature dependence of the hyperfine fields in $Dy_3Fe_5O_{12}$, see figure 5, does not reveal a sudden change in the hyperfine fields at the spin-reorientation temperature of 14 K. Hence, the orientation of the rare-earth magnetic moment has no significant influence on the iron magnetic hyperfine fields. The reduced 16a and 24d hyperfine fields in $Dy_3Fe_5O_{12}$ are shown in figure 6 as a function of the reduced temperature. In order to calculate the reduced values, the saturation hyperfine fields have been taken equal to their 4.2 K values and the Curie temperature has been taken equal to 550 K. In addition, the reduced 16a and 24d magnetizations in $Y_3Fe_5O_{12}$, measured [27] by neutron diffraction, have also been plotted in

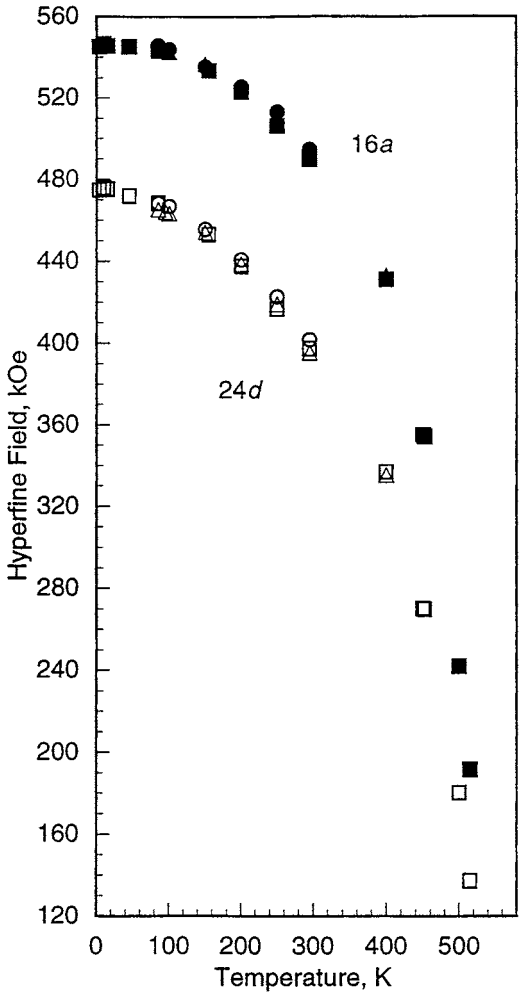

Figure 5. The temperature dependence of the 16a and 24d weighted average hyperfine fields in $R_3Fe_5O_{12}$, where R is Dy, ■, Eu, ●, and Y, ▲. The error bars are approximately the size of the data points.

figure 6 as open squares and open triangles. It is clear that the 24d reduced hyperfine field in $Dy_3Fe_5O_{12}$ and the 24d reduced magnetization in $Y_3Fe_5O_{12}$ agree quite well and follow the Brillouin function for $S = 5/2$, a function which is represented by the solid curve in figure 6. The similar behaviour of the 24d sites in $Dy_3Fe_5O_{12}$ and $Y_3Fe_5O_{12}$ indicates that the magnetic superexchange interactions at these sites are not influenced by the presence of a magnetic ion in the 24c dodecahedral site. In contrast, the 16a reduced hyperfine fields in $Dy_3Fe_5O_{12}$ and the 16a reduced magnetizations in $Y_3Fe_5O_{12}$ are larger than predicted by the Brillouin function for $S = 5/2$. This departure from the Brillouin curve has been attributed [27] to a small biquadratic exchange at the 16a sites rather than intrasublattice magnetic exchanges. The existence of a biquadratic exchange may play a role in the magnetocrystalline anisotropy of these garnets.

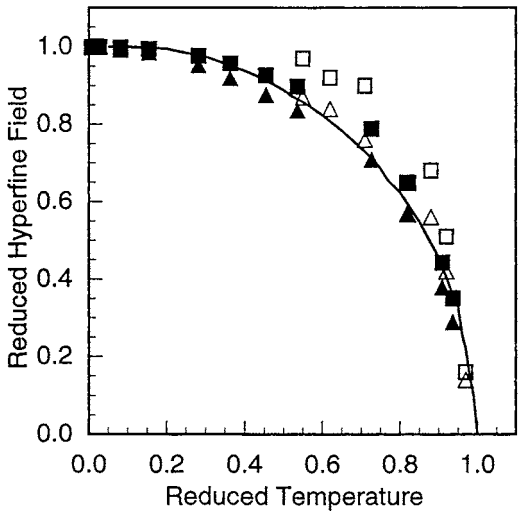

Figure 6. The reduced hyperfine field versus reduced temperature in $Dy_3Fe_5O_{12}$ for the 16a site, ■, and for the 24d site, ▲. The solid line is the Brillouin curve for $S = 5/2$. The open squares and triangles are the reduced sublattice magnetizations for $Y_3Fe_5O_{12}$ measured by neutron diffraction and taken from [27].

4.3. Isomer shifts

As indicated by the isomer shift values given in tables 1 and 2, the octahedral 16a isomer shifts are larger than the tetrahedral 24d isomer shifts at all temperatures. This difference, which is similar to that observed [26] in spinels, results from the increased 4s electron density at the tetrahedral 24d site, an increase which decreases the isomer shift.

The temperature dependence of the 16a and 24d isomer shifts in $Dy_3Fe_5O_{12}$ is shown in figure 7. Similar temperature dependences have been obtained for $Y_3Fe_5O_{12}$ and $Eu_3Fe_5O_{12}$ over a more restricted temperature range. In agreement with the second order Doppler shift, both isomer shifts decrease with increasing temperature. The solid line in figure 7 is a fit [28] of the temperature dependence of the isomer shifts within the Debye model of the lattice vibrations. It is well known [15] that the Debye model is at best an oversimplified model for describing the lattice vibrations of the complex garnet structure, but in the absence of a better model we will use it. In the fit shown in figure 7, for each site, two parameters were adjusted, an effective vibrating mass for the iron-57 nuclide and a Mössbauer temperature, i.e., the equivalent of the Debye temperature. The fitted values are 57 ± 1 g mol^{-1} and 405 ± 5 K and 505 ± 5 K for the 16a and 24d site, respectively. An effective vibrating mass of 57 ± 1 g mol^{-1} is indeed expected [29] for an iron(III) ion which is ionically bonded to its oxygen neighbours. These Mössbauer temperatures agree with the range of Debye temperatures measured [15] for $Y_3Fe_5O_{12}$, a range which extends from 454 to 599 K. The different Mössbauer temperatures for the 16a and 24d sites indicate different vibrational frequencies for these two sites. From the temperature dependence of the logarithm of the absorption area, i.e., the recoil-free fraction, in $Y_3Fe_5O_{12}$, Sawatzky *et al* [15] deduced Mössbauer temperatures of 366 ± 15 and 406 ± 15 K for the 16a and 24d sites, respectively. These values are significantly smaller than those measured herein from the temperature dependence of the isomer shifts in $Dy_3Fe_5O_{12}$. It is also well known [26] that different parts of the phonon spectrum of a solid are probed by the temperature dependence of the recoil-free fraction and of the isomer shift. Further, the tetrahedral 24d sites is characterized by a larger Mössbauer temperature than the octahedral 16a

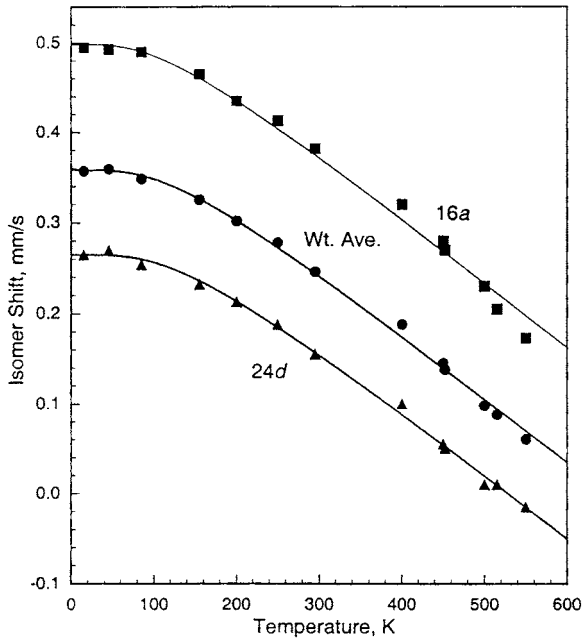

Figure 7. The temperature dependence of the 16a, ■, and 24d, ▲, isomer shifts in $Dy_3Fe_5O_{12}$. The solid lines are the result of a Debye model fit. The error bars are approximately the size of the data points.

site. A similar but smaller difference is observed [26] in the spinels, in which the tetrahedral sites are characterized by a Mössbauer temperature which is ∼20 K higher than that of the octahedral sites. This difference is usually attributed to the stronger Fe^{3+}–O^{2-} bond with a higher covalency at the tetrahedral site. As a consequence of this stronger bonding at the tetrahedral site, a difference between the recoil-free fractions of the tetrahedral and octahedral sites may be expected above room temperature but not below 85 K. Actually, between 4.2 and 550 K our fits, which assume equal recoil-free fractions for both sites, are excellent.

4.4. Quadrupole interactions

The values of ΔE_Q given in tables 1 and 2 correspond to $e^2Qq/2$, where e is the electronic charge, Q is the iron-57 nuclear quadrupole moment and eq is the principal component of the electric field gradient tensor. For the sake of simplicity, we will assume that the asymmetry parameter of the electric field gradient tensor is zero for both the 16a and 24d sites. This is not an assumption but must be true if the garnet space group is $Ia\bar{3}d$ at all temperatures and it is a valid assumption if the garnet space group is $R\bar{3}$ at temperatures below the Curie temperature, because the displacements [8, 25] of the ions involved in going from $Ia\bar{3}d$ to $R\bar{3}$ are very small. As indicated by the values given in table 1, the quadrupole interactions at both the 16a and 24d sites are independent of temperature between 15 and 295 K, for the three garnets studied herein. The sign of the quadrupole interaction at the 16a site is easily determined from the known values of the θ angles and is negative in agreement with earlier determinations [25]. The sign of the quadrupole interaction at the 24d site is more difficult to determine in the present study because the θ angles are distributed around the magic angle of 54.7°; however, a negative sign was reported previously [30]. Further, lattice point charge calculations [22] of the electric

field gradient at the 16a and 24d sites in the rare-earth iron garnets yield negative quadrupole interactions but they predict the largest quadrupole interaction on the 16a site. A significant contribution to the electric field gradient from the distortion of the filled metal orbitals by the oxygen dianions was suggested [31] to explain the large observed quadrupole interaction on the 24d site. We expect that this contribution would be enhanced by the rhombohedral distortion proposed herein.

The values of the θ angles for the 24d site are essentially temperature independent for the three garnets and their values suggest that the rhombohedral distortion of the site symmetry does not change between 15 and 295 K.

5. Conclusion

An analysis of the high resolution Mössbauer spectra of $R_3Fe_5O_{12}$, where R is Y, Eu and Dy, in their ferrimagnetic state reveals a rhombohedral distorsion of the lattice symmetry of these garnets. The existence of this distorsion is in agreement with an easy axis of magnetization which is oriented along the threefold axis of the unit cell. Further, the rhombohedral distorsion must be taken into account in the analysis and understanding of the magneto-optical properties of these garnets, properties which are very important for technological applications. In addition, our Mössbauer spectral study also reveals the presence of biquadratic exchange in the temperature dependence of the hyperfine fields and yields values for the lattice vibrational temperatures from the temperature dependence of the isomer shifts. Finally, this work has provided a basis for the study [32] of thin films of $Dy_3Fe_5O_{12}$.

Acknowledgments

This research was supported in part by the US National Science Foundation through grants DMR95-21739 and INT-9815138, the Ministère de la Communauté Française de Belgique through grant ARC 94-99/175 and the Fonds National de la Recherche Scientifique, Belgium. The authors thank Dr M Guillot, CNRS, Grenoble, France and Dr H Flack, University of Geneva, Switzerland, for fruitful discussions, Professors A Rulmont and P Tarte, for their help in preparing the samples, Professor A M Fransolet, Drs R Skumsky and G Van den Bossche, and Mr Joassin and Mr Swennen for their help in obtaining the x-ray diffraction patterns.

References

[1] Krumme J P, Doormann V, Hansen P, Baumgart H, Petruzello J and Viegers M P A 1991 *J. Appl. Phys.* **66** 4765
[2] Eppler W R and Kryder M H 1995 *J. Phys. Chem. Solids* **56** 1749
[3] Guillot M, Le Gall H and Leblanc M 1990 *J. Magn. Magn. Mater.* **86** 13
[4] Rodic D, Tellgren R and Guillot M 1991 *J. Magn. Magn. Mater.* **94** 260
[5] Geller S 1967 *Z. Kristallogr.* **125** 1
[6] Bertaut E F, Sayetat F and Tchéou F 1970 *Solid State Commun.* **8** 239
[7] Sayetat F 1975 *J. Appl. Phys.* **46** 3619
[8] Chenavas J, Joubert J C, Marezio M and Ferrand B 1978 *J. Less-Commn Met.* **62** 373
[9] Geschwind S 1961 *Phys. Rev.* **121** 363
[10] Geller S and Gilleo M A 1957 *J. Phys. Chem. Solids* **3** 30
[11] Geller S and Gilleo M A 1957 *Acta Crystallogr.* **10** 239
[12] Hansen P and Krumme J P 1984 *Thin Solid Films* **114** 69
[13] Guillot M 1995 *Materials Science and Technology* vol 3B, ed R W Cahn *et al* (New York: VCH) ch 8
[14] Aubert G and Michelutti B 1980 *J. Magn. Magn. Mater.* **19** 396
[15] Sawatzky G A, Van der Woude F and Morrish A H 1969 *Phys. Rev.* **183** 383
[16] Sankaranarayanan V K and Gajbhiye N S 1994 *J. Mater. Sci.* **29** 762

[17] Lataifeh M S and Lehlooh A D 1996 *Solid State Commun.* **97** 805
[18] Grenèche J M, Pascard H and Regnard J R 1988 *Solid State Commun.* **65** 713
[19] Winkler H, Eisberg R, Alp E, Rüffer R, Gerdau E, Lauer S, Trautwein A X, Grodzicki M and Vera A 1983 *Z. Phys.* B **49** 331
[20] Vandormael D 1999 *PhD Thesis* University of Liège
[21] Winkler G 1981 *Magnetic Garnets (Vieweg Tracts in Pure and Applied Physics, vol 5)* (Braunschweig: Vieweg) ch 2
[22] Stadnik Z M 1984 *J. Phys. Chem. Solids* **45** 311
[23] Berry F J, Davalos J Z, Ramon J, Greaves C, Marco J F, Slater P and Vithal M 1996 *J. Solid State Chem.* **122** 118
[24] Marest G, Perez A, Gérard P and Mackowski J M 1986 *Phys. Rev.* B **34** 4831
[25] Dong J and Lu K 1991 *Phys. Rev.* B **43** 8808
[26] Vandenberghe R E and De Grave E 1989 *Mössbauer Spectroscopy Applied to Inorganic Chemistry* vol 3, ed G J Long and F Grandjean (New York: Plenum) p 59
[27] Prince E J 1965 *Appl. Phys.* **36** 1845
[28] Long G J, Hautot D, Grandjean F, Morelli D T and Meisner G P 1999 *Phys. Rev.* B **60** 7410
[29] Herber R H 1984 *Mössbauer Spectroscopy* ed R H Herber (New York: Plenum) p 199
[30] Sawkicki J and Hafner S S 1978 *Phys. Rev.* A **68** 80
[31] Sawatzky G A and Van der Woude F 1969 *J. Physique Coll.* **35** C6 47
[32] Vandormael D, Grandjean J, Fleury-Frenette K and Delwiche J 2001 *IEEE Trans. Magn.* at press